Splitting Frequency Diversity in Wireless Power Transmission

Hoang Nguyen, *Student Member, IEEE*, and Johnson I. Agbinya

***Abstract*—This paper investigates the methodology to create multiple frequency modes in a multiresonator system of one transmitter and multiple receivers based on the circuit theory. The multiple frequencies from natural responses of magnetic couplings could be obtained by determining the eigenvalues of a matrix equation. This potentially allows us to diversify transmissions to and from devices. Theoretical calculations and experiments show similar results of the multiple frequencies at given coupling conditions. Models of two, three, and four coils in straight line demonstrate the splitting mode in the spectral domain, which are validated by envelopes of signals. In measurements, three frequencies of 525, 625, and 695 kHz, and four frequencies of 495, 590, 670, and 755 kHz are achieved at the receiver for three- and four-coil models, respectively, when coils are equally distanced by 2 cm. When coupling coefficient of every adjacent coil in three-coil model is 0.2, aggregating the peak power at two and three splitting modes result in 28% and 71%, respectively, more power than that at resonance frequency. Similarly, with two, three, and four modes in four-coil model, the increases are 43%, 23%, and 33% with two, three, and four modes, respectively.**

***Index Terms*—Multiple resonators, splitting frequency, wireless power transfer.**

I. Introduction

DEVELOPMENTS in near-field strongly coupled magnetic resonances of the MIT group in 2007 have led to a renewed interest in research in wireless power transfer [1]. In their experiment, power is wirelessly transferred from a source coil to a load coil at a distance that is three times larger than the radius of the coil. Using strong coupling of two resonators, the system lights up a 60-W light bulb with a 40% efficiency. The advantages of the MIT experiment include the flexible position of the transmitter and receiver coil and the high power efficiency at the longer distance (middle-range) between the coils. There are potential applications developed from this experiment such as cordless battery chargers in mobile phones [2], [3], vehicles [4]–[6], implant devices [7], [8], underground sensor network [9], and internet of things [10]. The use of the relay coil to extend the transmission range and energy efficiency is also studied in three- and four-coil models [11], [12] and multiple coils [8], [13]–[16]. The effects of the magnetic couplings of adjacent and nonadjacent coils have recently been examined for multiple coils in domino system [13], multiple transmitter coils [17], [18], and multiple receiver coils [18], [19].

Many factors influence the induced magnetic flux in the receiver coil including quality factors (Q), efficiencies of the coils, the coil dimensions, mutual inductance, and also the distance between the coils. This can be quantified in terms of the received power in [20]. Fluxes from the transmitting inductive coil are picked up by the receiving coil via mutual inductance and, hence, induce a current in the receiver load. However, the degree of the flux couplings between two coils can lead to a splitting frequency with a negative effect on the received power [18]. There has been a strong research focus on the splitting frequency [21]–[24]. Nevertheless, none examined the use of the splitting mode for transmission in the multiresonant system. In a pair of magnetically coupled coil resonators, when the transmitter and receiver are placed so close to each other that the coupling condition is greater than the critical coupling, the single resonant peak at the load of the receiver splits to double peaks. This phenomenon is known as the splitting frequency. Moreover, the double peaks vary with different coupling points below the critical condition. In other words, the variation of the distance between the transmitter and receiver within the range below the critical point is the prerequisite for the multiplicity of the splitting frequencies. The common approach is to ignore the splitting behavior by using the impedance matching technique [2] or the adaptive shifting frequency [2], [17], [25] to overcome the degradation of power efficiency. This paper, however, utilizes and employs frequency splitting as an advantageous phenomenon to diversify to the multiple receivers.

The effects of the magnetic flux in terms of the coupling coefficient are investigated in [17] and [26] for multiple receivers. The effective frequencies should be set at the driving frequency that maximizes power transfer for a given coupling between the receivers. However, Ahn *et al.* [17] limited their study to the case of equal coupling between the receivers and the weak coupling from the transmitter to the receivers. Ahn *et al.* [26] also studied the effects of the coupling on power efficiency in three- and four-coil systems and point out that the frequency should be adjusted or the repeaters should be correctly positioned to obtain maximum power transfer. However, the use of splitting frequency modes for each resonator is not considered. This paper examines the discussion on mode splitting for the coupling interaction between transmitter to N receivers in the straight domino-resonators.

Using matrix calculus, Karaca *et al*. [27] confirms the presence of a set of specific eigenmodes in multiresonant systems. However, the eigenvalues in [27] are merely calculated with the adjacent neighbors and the eigenfrequencies based on the coupling coefficient are not shown. Additionally, they do not use eigenfrequencies to diversify the transmissions. We examine the different splitting frequencies under various coupling

Manuscript received September 30, 2014; revised February 26, 2015; accepted April 7, 2015. Date of publication April 20, 2015; date of current version July 10, 2015. Recommended for publication by Associate Editor J. T. Boys.

The authors are with the Department of Electronic Engineering, La Trobe University, Bundoora, Vic. 3086, Australia, and also with the School of Information Technology and Engineering, Melbourne Institute of Technology, Melbourne, Vic. 3000, Australia (e-mail: nghoang_98@yahoo.com; jagbinya@mit.edu.au).

Color versions of one or more of the figures in this paper are available online at http://ieeexplore.ieee.org.

Digital Object Identifier 10.1109/TPEL.2015.2424312

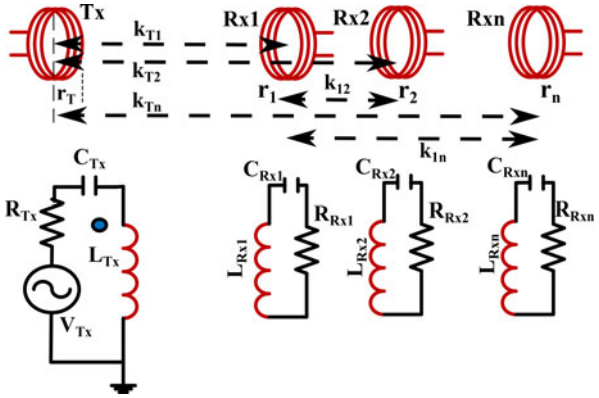

Fig. 1. Single transmitter (Tx) and multiple receivers (Rx_i).

conditions and provide more accurate localization of the exact split frequencies by solving the system of eigenvalue equations. The adapted distances and the strength of the coupling corresponding to the multiple frequencies are shown and validated. The rest of this paper is presented as follows. Section II introduces the theory of splitting frequency for *N* mode splitting frequencies in configuration of transmitter-*N* receivers. Section III classifies splitting modes for three- and four-coil models. The simulation results of three- and four-coil models are presented in Section IV. The experimental evaluation of mode splitting for one, two, and three receivers are included in Section V. Power improvement is demonstrated in Section VI. The last section is our conclusion.

II. Methodology Model of Transmitter–Multiple Receivers

The aim of this section is to investigate the splitting frequency in terms of eigenvalues for an excitation source of *N* coil configuration. For this purpose, we derive the matrix equation based on the circuit theory in [17] and [27]. The distinctive splitting frequencies are introduced according to a variety of coupling conditions. Fig. 1 shows the model of a transmitter and *N* receivers in a domino form. The mutual inductance among the receivers and between the transmitter and *N* receivers are called M_{ij} and $M_{Ti}(i = 1 : N,\ j = 1 : N$ and $i \neq j)$, respectively. When a voltage source of transmitter V_{Tx} is turned ON, the magnetic fluxes from the transmitter induce currents at the *N* receiver loops. The currents in each resonator are denoted as $I_{Tx}, I_1, I_2, \ldots I_N$. The impedance of resonators are represented by $Z_{Tx} = R_{Tx} + j\omega L_{Tx} + \frac{1}{j\omega C_{Tx}}$ and $Z_i = R_i + j\omega L_i + \frac{1}{j\omega C_i}$ (with $i = 1 : N$), where *R*, *L*, and *C* are the resistance, inductance, and capacitance, respectively, in each resonator. According to the Kirchhoff voltage law, the transmitter and *N* receivers relate through the following matrix:

$$\begin{vmatrix} Z_{Tx} & j\omega M_{T1} & j\omega M_{T2} & \cdots & j\omega M_{Tn} \\ j\omega M_{T1} & Z_1 & j\omega M_{12} & \cdots & j\omega M_{1n} \\ j\omega M_{T2} & j\omega M_{12} & Z_2 & \cdots & j\omega M_{2n} \\ \vdots & \vdots & \vdots & \cdots & \vdots \\ j\omega M_{Tn} & j\omega M_{1n} & j\omega M_{2n} & \cdots & Z_N \end{vmatrix} \begin{vmatrix} I_{Tx} \\ I_1 \\ I_2 \\ \vdots \\ I_N \end{vmatrix} = \begin{vmatrix} V_{Tx} \\ 0 \\ 0 \\ \vdots \\ 0 \end{vmatrix}. \tag{1}$$

It is noticed that the cross coupling and directed-coupling coefficients (k_{ij} and k_{Ti}) can be calculated by the mutual inductance between the coils and their self-inductances as $k_{ij} = \frac{M_{ij}}{\sqrt{L_i L_j}}$ *and* $k_{Ti} = \frac{M_{Ti}}{\sqrt{L_{Tx} L_i}}$ $(i, j = 1 : N$ and $i \neq j)$. The inductor factors are defined as $a_i = \sqrt{\frac{L_i}{L_{Tx}}}(i = 1 : N)$ and $a_{ij} = \sqrt{\frac{L_i}{L_j}}(i, j = 1 : N$ and $i \neq j)$. The transformed impedances are called Z'_{Tx} and Z'_i, where $Z'_{Tx} = \frac{R_{Tx}}{j\omega L_{Tx}} + (1 - \frac{\omega_o^2}{\omega^2})$ and $Z'_i = \frac{R_i}{j\omega L_i} + (1 - \frac{\omega_o^2}{\omega^2})$ (with $i = 1 : N$), and the resonant frequency $\omega_o = \frac{1}{\sqrt{LC}}$. Equation (1) can be rewritten as follows:

$$\begin{vmatrix} Z'_{Tx} & k_{T1}a_1 & k_{T2}a_2 & \cdots & k_{Tn}a_n \\ k_{T1}a_1^{-1} & Z'_1 & k_{12}a_{12} & \cdots & k_{1n}a_{1n} \\ k_{T2}a_2^{-1} & k_{12}a_{12}^{-1} & Z'_2 & \cdots & k_{2n}a_{2n} \\ \vdots & \vdots & \vdots & \cdots & \vdots \\ k_{Tn}a_n^{-1} & k_{1n}a_{1n}^{-1} & k_{2n}a_{2n}^{-1} & \cdots & Z'_N \end{vmatrix} \begin{vmatrix} I_{Tx} \\ I_1 \\ I_2 \\ \vdots \\ I_N \end{vmatrix} = \begin{vmatrix} \frac{V_{Tx}}{j\omega L_{Tx}} \\ 0 \\ 0 \\ \vdots \\ 0 \end{vmatrix}. \tag{2}$$

Determination of Splitting Frequency: It is reported in [17] that the imaginary part $j\omega L$ of the transformed impedance in resonators greatly exceeds the real part *R* in magnitude under a critical coupling condition and high-quality factor ($Q = \frac{\omega L}{R}$). Therefore, the factor $\frac{R}{\omega L}$ and $\frac{V_{Tx}}{j\omega L_{Tx}}$ become negligible. Equation (2) can be transformed into $A * \bar{I} = \frac{\omega_0^2}{\omega^2} * \bar{I}$ with the vector current $\bar{I} = (I_{Tx}, I_1, I_2 \ldots I_N)^T$ and matrix A

$$A = \begin{vmatrix} 1 & k_{T1}a_1 & k_{T2}a_2 & \cdots & k_{Tn}a_n \\ k_{T1}a_1^{-1} & 1 & k_{12}a_{12} & \cdots & k_{1n}a_{1n} \\ k_{T2}a_2^{-1} & k_{12}a_{12}^{-1} & 1 & \cdots & k_{2n}a_{2n} \\ \vdots & \vdots & \vdots & 1 & \vdots \\ k_{Tn}a_n^{-1} & k_{1n}a_{1n}^{-1} & k_{2n}a_{2n}^{-1} & \cdots & 1 \end{vmatrix}. \tag{3}$$

The natural modes of the system can be obtained by solving for the eigenvalues of the matrix A in (3). The modes represent the natural response of the system under no excitation. Hence, they provide the best response frequencies of the system. The magnitude and phase of these modes are also given by the eigenvectors of the matrix *A*. To simplify the mathematical model, we assume that the self-inductances of the resonators are the same $L_{Tx} = L_i = L_j$, which means the inductor factors (a_i and a_{ij}) are equal to 1. Thus, it allows (3) to be transformed into the following matrix:

$$B = \begin{vmatrix} 1 & k_{T1} & k_{T2} & \cdots & k_{Tn} \\ k_{T1} & 1 & k_{12} & \cdots & k_{1n} \\ k_{T2} & k_{12} & 1 & \cdots & k_{2n} \\ \vdots & \vdots & \vdots & 1 & \vdots \\ k_{Tn} & k_{1n} & k_{2n} & \cdots & 1 \end{vmatrix}. \tag{4}$$

It is noticed that eigenvalues λ of (4) resulting in splitting frequencies are the roots of the nth degree equation. By definition, they can be obtained by solving the determinant of $B - \lambda I = 0$, where I is identity matrix. Furthermore, it is observed that the

only factor affecting the mode splitting phenomenon is the coupling coefficients. However, the coupling coefficient can be calculated from radii of the two adjacent coils r_i, r_j and the distance d between them as $k_{ij}^2 = \frac{r_i^3 r_j^3 \pi^2}{(d^2+r_i^2)^3}$ [20], [28]. Therefore, it is true that the degree of a flux condition between the coils determines the splitting mode, which confirms that splitting frequency as the result of the natural response of inductive systems. The conventional resonant frequency ω_o does not decide the modes, but alters the magnitudes of the splitting frequencies due to its relationship with the eigenvalues and these frequencies. In addition, from (4), the splitting frequencies of the system could be accurately estimated, since we can measure the geometrical dimension of coils and distance between them. Actually, we need to find only distance (variable value) since the radii of coils are known. This method is demonstrated in Section V.

Determination of Current and Power Transfer: With specific input voltage at the transmitter, the current of each resonator in (2) can be obtained by the following equation:

$$I_i = A^{-1}V = \frac{VA^T}{\det(A)} \, (i = Tx, 1, \dots N) \tag{5}$$

where voltage vector $V = (\frac{V_{Tx}}{j\omega L_{Tx}}, 0, \dots 0)^T$. $\det(A)$ is the determinant of the matrix *A* and A^T is the transpose matrix.

It is noticed that the receiver voltage across the load is equal to $V_i = -I_i R_i$ and the relationship between the voltages of transmitter and receiver is given as $\frac{V_i}{V_{Tx}}$. Therefore, the magnitude of S_{21} can be calculated as follows:

$$S_{21} = 2\frac{V_i}{V_{Tx}}\sqrt{\frac{R_i}{R_{Tx}}}. \tag{6}$$

The parameter S_{21} refers to the ratio of signal measured at an output port of the receiver to the signal incident at an input port of the transmitter. This parameter is vital to power transfer as its squared root ($|S_{21}|^2$) represents the power gained at the receiver. In other words, this parameter quantifies the efficiency of power transfer. Furthermore, from (5), the power transfer between the *N* resonators and the transmitter can be expressed by the equation

$$\frac{Pi}{P_{Tx}} = \left|\frac{I_i}{I_{Tx}}\right|^2 \frac{R_i}{R_{Tx}} \, (i = 1 : N). \tag{7}$$

III. Classification of Splitting Modes for Three- and Four-Coil Models

The method of splitting frequency is applied to three- and four-coil models. Assume that the transmitter and receiver have similar impedances ($Z_{Tx} = Z_i = Z$) and self-inductances.

1) One Transmitter and Two Receivers (SI2O): Applying (4), we can rewrite the expression for the SI2O system as the 3×3 matrix below:

$$\begin{vmatrix} 1 & k_{T1} & k_{T2} \\ k_{T1} & 1 & k_{12} \\ k_{T2} & k_{12} & 1 \end{vmatrix} \overline{I} = \frac{\omega_0^2}{\omega^2}\,\overline{I}. \tag{8}$$

1) *Case 1:* When $k_{T1} = k_{12} = k$ and $k_{T2} = 0$, three splitting frequencies are solved from (8) as $\omega_1 = \omega_o$ and $\omega_2 = \omega_3 = \frac{\omega_o}{\sqrt{1\pm k\sqrt{2}}}$ $(0 < k < 0.7)$. Insert the coupling coefficient into (5), the current of each resonator is derived as

$$I_{Tx} = \frac{V(Z^2-k^2)}{Z(Z^2-2k^2)},\; I_1 = \frac{-Vk}{Z^2-2k^2},\; I_2 = \frac{Vk^2}{Z(Z^2-2k^2)}. \tag{9}$$

It is observed that the equations show different splitting frequencies in each receiver. Receiver 1 has two frequencies ω_2 and ω_3, while receiver 2 has three frequencies ω_1, ω_2, and ω_3.

1) *Case 2:* when $k_{T1} = k_{12} = k$ and $k_{T2} = m * k \, (0 < m < 1)$, three splitting frequencies and currents are obtained as follows: $\omega_1 = \frac{\omega_o}{\sqrt{1-mk}}$ and $\omega_2 = \omega_3 = \frac{\omega_o}{\sqrt{\frac{mk}{2} \pm \frac{k\sqrt{m^2+8}}{2}+1}}$,

$$I_{Tx} = \frac{V(Z^2-k^2)}{(Z-mk)\left(Z+\frac{mk}{2}+\frac{k\sqrt{m^2+8}}{2}\right)\left(Z+\frac{mk}{2}-\frac{k\sqrt{m^2+8}}{2}\right)}$$

$$I_1 = -\frac{Vk}{\left(Z+\frac{mk}{2}+\frac{k\sqrt{m^2+8}}{2}\right)\left(Z+\frac{mk}{2}-\frac{k\sqrt{m^2+8}}{2}\right)}$$

$$I_2 = -\frac{Vk(k-Zm)}{(Z-mk)\left(Z+\frac{mk}{2}+\frac{k\sqrt{m^2+8}}{2}\right)\left(Z+\frac{mk}{2}-\frac{k\sqrt{m^2+8}}{2}\right)}.$$

Again, the current equation shows that the power at receivers 1 and 2 is maximized at two and three frequencies, respectively.

1) *Case 3:* When $k_{T1} = k_{T2} = k_{12} = k$, the transmitter and two receivers are not on a straight line. Two splitting frequencies and currents are obtained as follows: $\omega_2 = \frac{\omega_o}{\sqrt{1-k}}$ and $\omega_3 = \frac{\omega_o}{\sqrt{1+2k}}$,

$$I_{Tx} = \frac{V(Z+k)}{(Z-k)(Z+2k)},\; I_1 = I_2 = \frac{-Vk}{(Z-k)(Z+2k)}. \tag{10}$$

Two receivers have a similar splitting frequency ω_2 and ω_3.

2) One Transmitter and Three Receivers (SI3O): The similar method is applied to this configuration to calculate the splitting frequency

$$\begin{vmatrix} 1 & k_{T1} & k_{T2} & k_{T3} \\ k_{T1} & 1 & k_{12} & k_{13} \\ k_{T2} & k_{12} & 1 & k_{23} \\ k_{T3} & k_{13} & k_{23} & 1 \end{vmatrix} \overline{I} = \frac{\omega_0^2}{\omega^2}\,\overline{I}. \tag{11}$$

1) *Case 1:* When $k_{T1} = k_{T2} = k_{T3} = k$ and $k_{12} = k_{13} = k_{23} = 0$, the transmitter and three receivers in this situation are not on a straight line. Three splitting frequencies and currents are yielded from (11) as follows: $\omega_1 = \omega_o$ and $\omega_2 = \omega_3 = \frac{\omega_o}{\sqrt{1\pm k\sqrt{3}}}$ $(0 < k < 0.57)$

$$I_{Tx} = \frac{-VZ}{Z^2-3k^2},\; I_1 = I_2 = I_3 = \frac{-Vk}{Z^2-3k^2}. \tag{12}$$

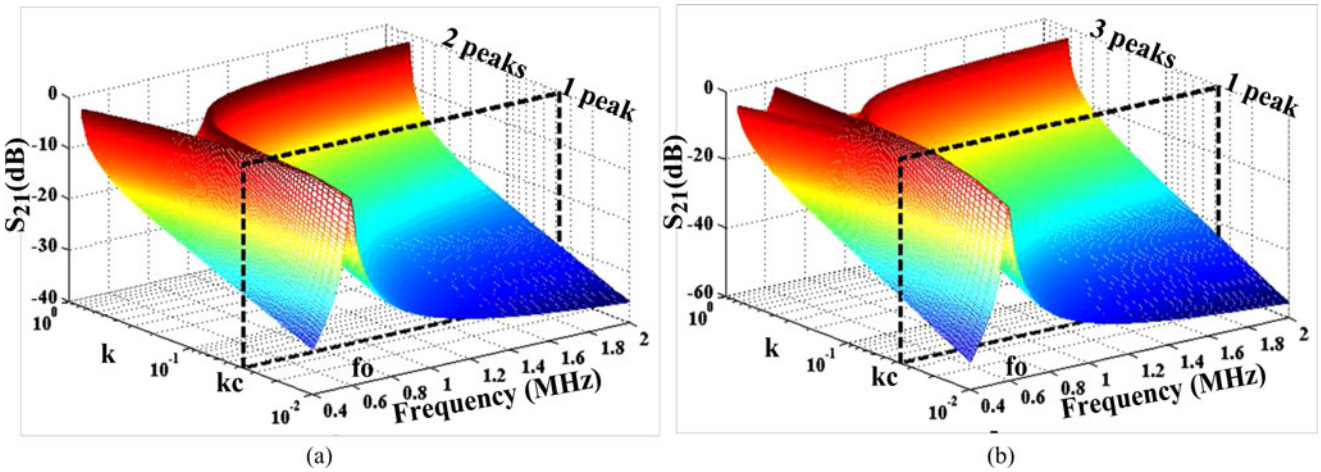

Fig. 2. Three-coil system without the cross coupling between the transmitter and receiver 2. (a) and (b) are for receivers 1 and 2, respectively.

The power at the receivers is maximized at the frequencies of ω_2 and ω_3.

1) *Case 2:* When $k_{T1} = k_{12} = k_{23} = k$ and $k_{T2} = k_{T3} = k_{13} = 0$, four splitting frequencies and currents are obtained as follows: $\omega_{1,2} = \frac{\omega_o}{\sqrt{1 \pm k(\frac{\sqrt{5}+1}{2})}}$ and $\omega_{3,4} = \frac{\omega_o}{\sqrt{1 \pm k(\frac{\sqrt{5}-1}{2})}}$ $(0 < k < 0.6)$

$$I_{Tx} = -\frac{V(2Zk^2 - Z^3)}{\sigma}, \quad I_1 = -\frac{Vk(Z^2 - k^2)}{\sigma}$$
$$I_2 = -\frac{VZk^2}{\sigma}, \quad I_3 = -\frac{Vk^3}{\sigma} \tag{13}$$

where $\sigma = (Z \pm k(\frac{\sqrt{5}+1}{2}))(Z \pm k(\frac{\sqrt{5}-1}{2}))$. The results show that under a particular coupling condition, the system generates different splitting frequencies at the receiver.

IV. Simulation Results

The verification of multiple frequencies resulting from the effect of the coupling condition is introduced in this section. A possible approach is to analyze the performance of the system with power transfer equation. Thus, the magnitude of S_{21} in (6) as the function of the coupling coefficient and the frequency is simulated for three- and four-coil models. The circuit elements of the transmitter and receiver have the coil inductance of 7.3 μH and the capacitance of 10 nF. This produces the resonant frequency of $f_o = 590$ kHz. Note that the critical coupling k_c in the simulation is proportional to the quality factor of the coil as [17], [18] $k_c = \frac{1}{\sqrt{Q_i Q_j}}$ $(i, j = 1 : N$ and $i \neq j)$.

The 3-D view of S_{21} for the three-coil models in case 1 of the SI2O is plotted in Fig. 2. It is observed that at any coupling smaller than the critical point, both receivers 1 and 2 have only one frequency peak. However, at any coupling coefficient that is larger than the critical point, the two and three splitting frequencies exist at receivers 1 and 2, respectively. It is noticed that this situation happens when the coupling between Tx-Rx1 and Rx1-Rx2 are equal. This simulated result supports the formula we developed for the current at the receiver in (9). Fig. 2 also demonstrates that if the transmitter operates at the original resonant frequency f_o and $k > k_c$, the receiver 2 power is not affected as seen from graph (b), whereas the receiver power 1 is significantly reduced [graph (a)].

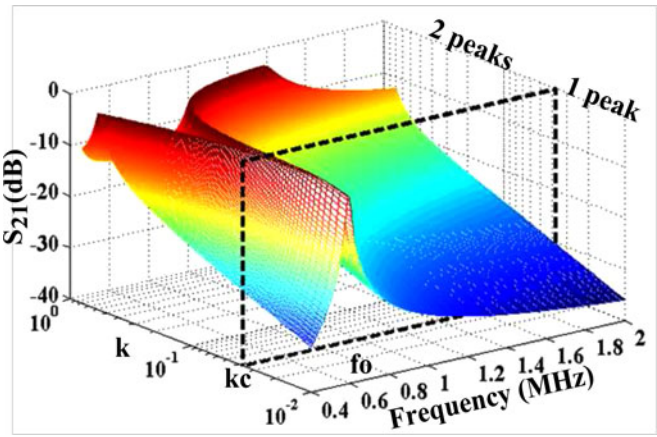

Fig. 3. S_{21} of receivers 1 and 2 in a three-coil models with the cross coupling.

Fig. 3 illustrates S_{21} of receivers 1 and 2 in case 3 of the SI2O model. It can be seen that both receivers 1 and 2 have an identical response of S_{21} at any coupling coefficient. This is true since the currents at receivers 1 and 2 [as in (10)] are similar. Furthermore, only two modes of frequency are also shown at the receiver 2 (see Fig. 3) instead of three modes in Fig. 2. Thus, the cross coupling affected the power received by the receiver 2 at the resonant frequency.

Two cases of the SI3O models are shown in Fig. 4. It is observed that two and four modes of splitting frequency are obtained for the cases 1 and 2 as in (12) and (13), respectively.

V. Experimental Evaluation for Multiple Modes

In this section, hardware experiments are conducted in both time and frequency domains. The models of two-, three-, and four-coils in straight resonator form are used to evaluate the multiple modes of frequency in inductive system. A single source with a swept frequency from 400 kHz to 2 MHz is provided to the proposed models. Fig. 5 shows the experimental setup measured by Tektronix TDS 2024B. The word "lobe" and "peak" are used to refer to the envelopes of the signals in the time domain and the maximum values of the frequency response, respectively. Identical Helmholtz coil is designed with the radius

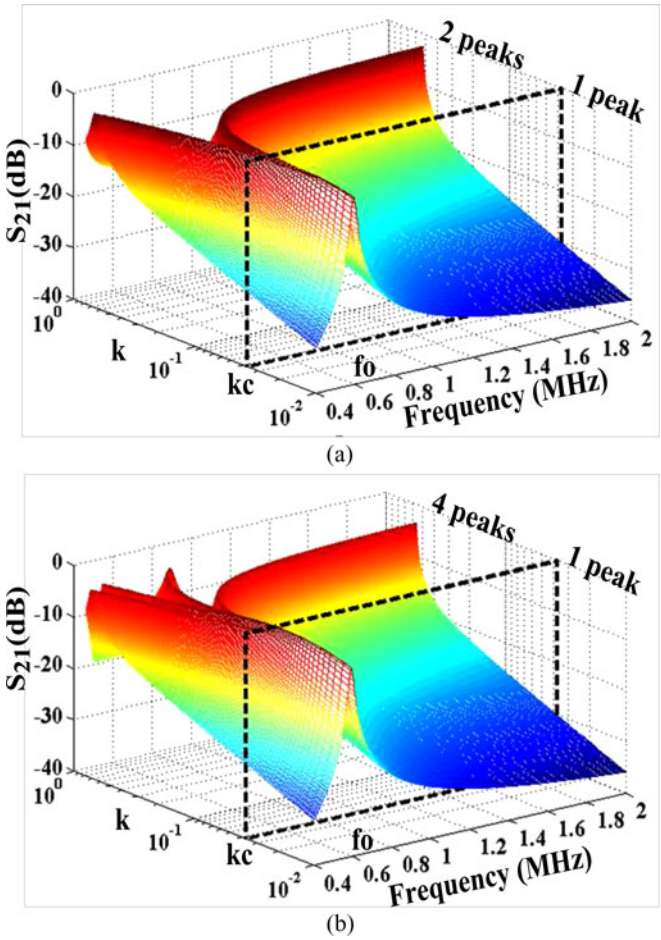

Fig. 4. S_{21} of receivers 1, 2, and 3 in four-coil system. (a) and (b) is cases 1 and 2, respectively.

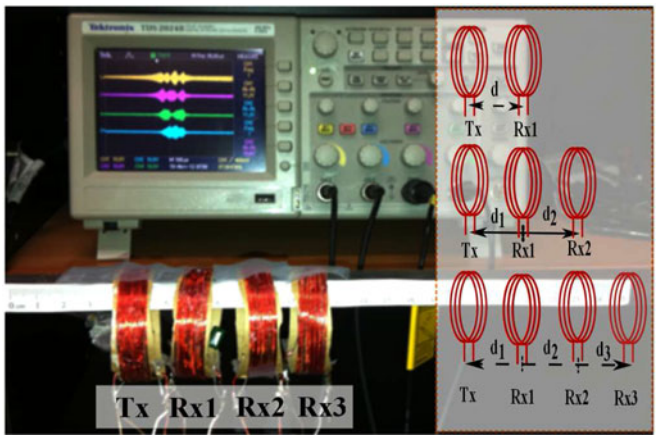

Fig. 5. Experimental system is arranged for two-, three- and four-coil models, respectively.

of 2.1 cm and the width of 0.8 mm, and the number of turns is 11. The coil is hand wound on a brown paper core. According to Wheeler's formula [29], the inductance of the coil is 7.3 μH. The ceramic capacitor of 10 nF is added in parallel to the coil. The parasitic resistance is 1 Ω. The unloaded quality factor Q of the coil is 27. Theoretically, resonant frequency is 590 kHz. Since it is required to have a high Q, the load resistance is chosen to be 1 Ω. With high-load resistance, higher resonant frequency or large inductor has to be designed.

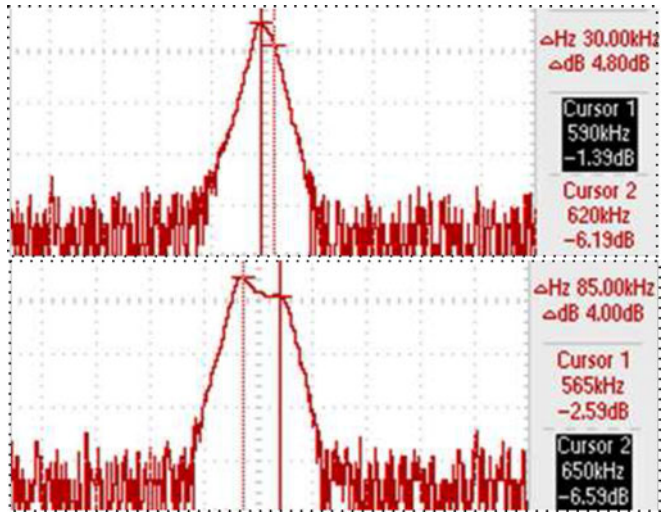

Fig. 6. Spectrum of two-coil system at $k = 0.01$ and 0.07.

TABLE I
TWO-COIL SYSTEM

d (cm)	k	f_1 (kHz)	f_2 (kHz)	f_o (kHz)
4	0.0101	590		
2.5	0.1392		565	650
			553*	636*
2	0.202		550	675
			538*	660*

* denotes for simulation results.

Model $N = 2$: For the two-coil system, the signal generator is connected to the transmitter coil and two channels of oscilloscope are linked to the transmitter and receiver coils. The gap between the transmitter and receiver is varied within 4 cm. The coupling coefficient between the two coils is a function of the physical dimension of the coils and the distance between them. The frequency spectrum at the receiver is demonstrated in Fig. 6. The details of frequency changes corresponding to the separation and the coupling coefficient k are introduced in Table I. It is observed that the spectral response changes from one to two frequencies as the distance (d) between the transmitter and receiver is reduced. At loose coupling $k = 0.01$, the receiver signal peaks at 590 kHz, which is the same resonant frequency. We can see that the conventional resonant frequency is the same between practice and theory. At $k = 0.1392$, two frequencies (565 and 650 kHz) are shown.

To evaluate the effect of splitting frequency on the power transfer, an excitation voltage is generated for a variety of coupling between the transmitter and receiver. Fig. 7 shows the waveform of the transmitter and receiver at the distance of 4 and 2.5 cm, respectively. It can be seen that the envelope of the signals has the same shape in both transmitter (at the top graph) and receiver (at the bottom graph). The envelope of the transmitter and receiver changes from one lobe to two lobes as the distance decreases to strong coupling coefficient. This explains that the circuit has single and double frequency responses. This also demonstrates that the splitting modes affect the maximum power transfer between the transmitter and receiver at the original resonant frequency.

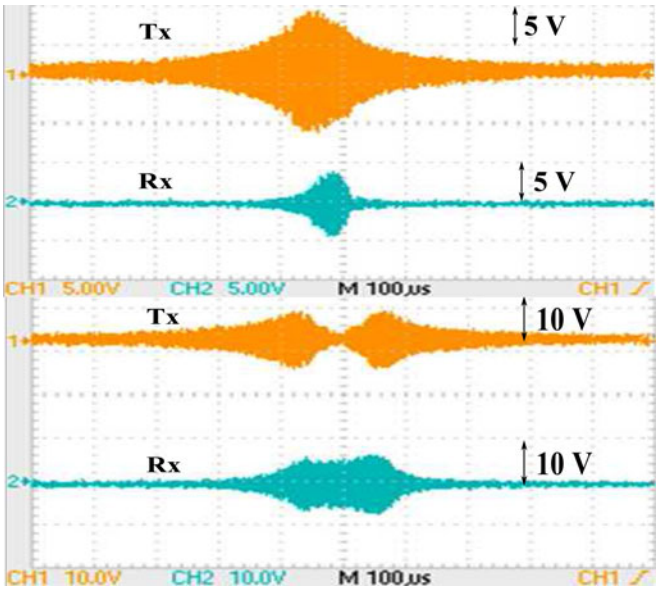

Fig. 7. Transmitter and receiver at different distances 4 and 2.5 cm.

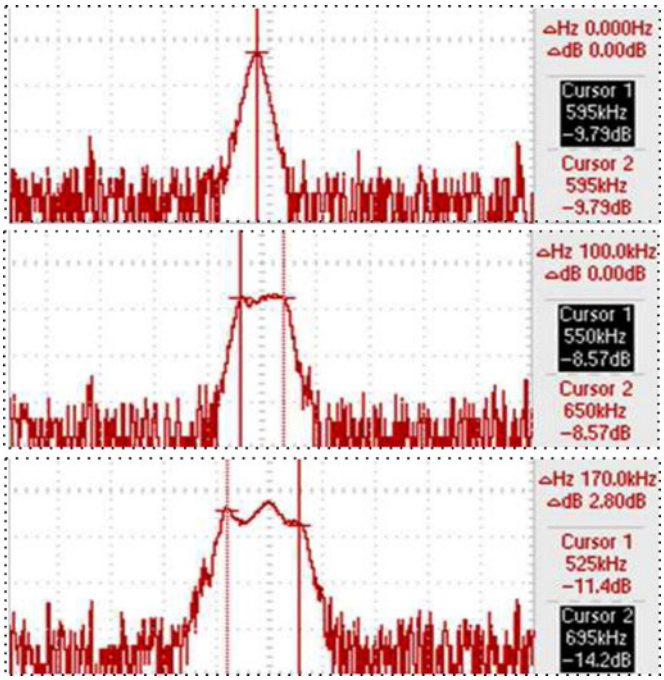

Fig. 8. Receiver 2 spectrum at different modes.

TABLE II
FREQUENCY OF RECEIVER 2 IN THREE-COIL MODEL

d_1 (cm)	d_2 (cm)	f_1 (kHz)	f_2 (kHz)	f_3 (kHz)
3.5	5.5	595		
3.5	2.5		550	650
			551*	638*
4	3		560	635
			573*	617*
2	2	625	525	695
		590*	476*	719*
2	1.5	615	535	685
		586*	406*	792*

d_1 and d_2 are the gap arrangement Tx-Rx1 and Rx1-Rx2, respectively.
* denotes for simulation results.

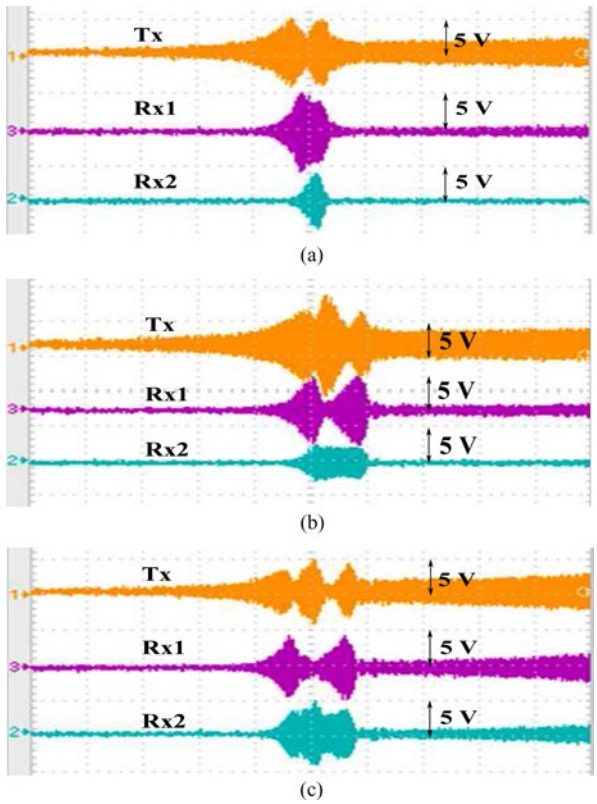

Fig. 9. Envelopes of signals in three-coil system. (a) refers to $k_{T1} = 0.0185$ and $k_{12} = 0.0021$. (b) refers to $k_{T1} = 0.0185$ and $k_{12} = 0.0708$. (c) refers to $k_{T1} = 0.144$ and $k_{12} = 0.144$..

Model $N = 3$: The method to determine the frequency splitting of the three-coil systems is the same as that with the two-coil system. In this experiment, we analyze the effect of the nonadjacent resonator on the transmitter and receiver. The frequency response at the load Rx2 is reported in Fig. 8 and Table II. It is shown that one, two, and three modes of frequencies can be obtained by proper arrangements of Rx1 and Rx2. At distance d_1(Tx-Rx1) $= 3.5$ cm and d_2(Rx1-Rx2) $= 5.5$ cm, one peak is found at the load Rx2. At the short distance of $d_1 = 3.5$ cm and $d_2 = 2.5$ cm, there are two frequencies (550 and 650 kHz) at Rx2. However, when Rx1 is separated 2 cm away from the transmitter and Rx2 $d_1 = d_2 = 2$ cm, we have three frequencies of 525, 625, and 695 kHz at Rx2. Table II also indicates that in three-coil model, ten frequencies (525–695 kHz) are achieved at Rx2 with four different coupling cases.

The voltage at different modes of resonators is illustrated in Fig. 9. In each figure, the transmitter, receiver 1, and receiver 2 signals are represented in the following order of top, middle, and bottom graphs, respectively. It is seen that the Rx2 signal has one, two, or three lobes, while the Rx1 signal has only two lobes. It means that the Rx1 and Rx2 signals are split into one, two, or three peaks regarding the given lobes. Additionally, two lobes of Rx1 due to the coupling between receivers and three lobes of Rx2 depend on the strong coupling between Tx1-Rx1 and Rx1-Rx2. Fig. 9(c) refers to the case when the coupling coefficient between Tx-Rx1 and Rx1-Rx2 are similar

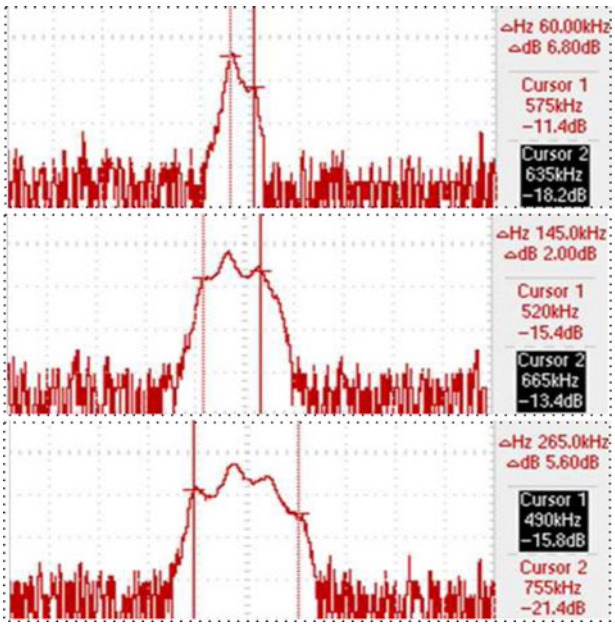

Fig. 10. Spectrum of receiver 3.

$(k_{T1} = k_{12} = 0.144)$. The voltage at the receivers 1 and 2 shows two and three lobes, respectively. This situation is proven in Section III by the equation of the receiver currents obtained in case 2 of the SI2O model.

Model $N = 4$: The third coil is inserted between the transmitter and two other receivers. The coil positions are also varied to see how the frequency response of the receiver changes. Fig. 10 and Table III show the spectral response at the receiver 3. It is seen that two, three, and four frequencies are created regarding the arrangement of the coils. At $d_1 = 3\,\text{cm}$, $d_2 = 5.5\,\text{cm}$, and $d_3 = 3.5\,\text{cm}$, two peaks are obtained 575 and 635 kHz. At $d_1 = d_2 = d_3 = 2\,\text{cm}$, four peaks are 495, 590, 670, and 755 kHz. As a result, Table III demonstrates that multiple frequencies are achieved by a proper arrangement of the coils obtained from model equations. With three different coupling cases, nine frequencies are obtained at Rx3. This creation of multiple frequencies can be used for frequency diversity of the inductive system. However, in device to device systems which need to operate at very short distances between transmitter and receiver, the two peaks could be counterproductive. For such situations, impedance matching should be used to force only one peak.

Time domain signals at three different cases are shown in Fig. 11. The transmitter and three receiver signals are from the top to bottom graphs, which refer to channels 1, 3, 4, and 2 of the oscilloscope, respectively. One and four lobes are obtained in Rx1, while two, three, and four lobes are presented in Rx2 and Rx3. For example, Fig. 11(c) refers to the case of four response frequencies when we have two strong coupling coefficients. The coupling coefficients are $k_{T1} = 0.144,\ k_{12} = 0.29,$ and $k_{23} = 0.54$. The output voltage also has four lobes representing the four peaks in the frequency domain. In fact, this case can be explained by case 2 of the SI3O model.

VI. Power Improvement

Although the split frequency phenomenon has been seen as counterproductive in wireless power transfer, in this paper,

TABLE III
Frequency of Receiver 3 in Four-Coil Model

d_1 (cm)	d_2 (cm)	d_3 (cm)	f_1 (kHz)	f_2 (kHz)	f_3 (kHz)	f_4 (kHz)
3	5.5	3.5	575	635		
			573*	616*		
2	2.5	2	525	580	665	
			525*	590*	543*	
2	2	2	495	590	670	755
			456*	541*	648*	734*

d_1 d_2 and d_3 are the gap arrangement Tx-Rx1, Rx1-Rx2, and Rx2-Rx3, respectively.
* denotes for simulation results.

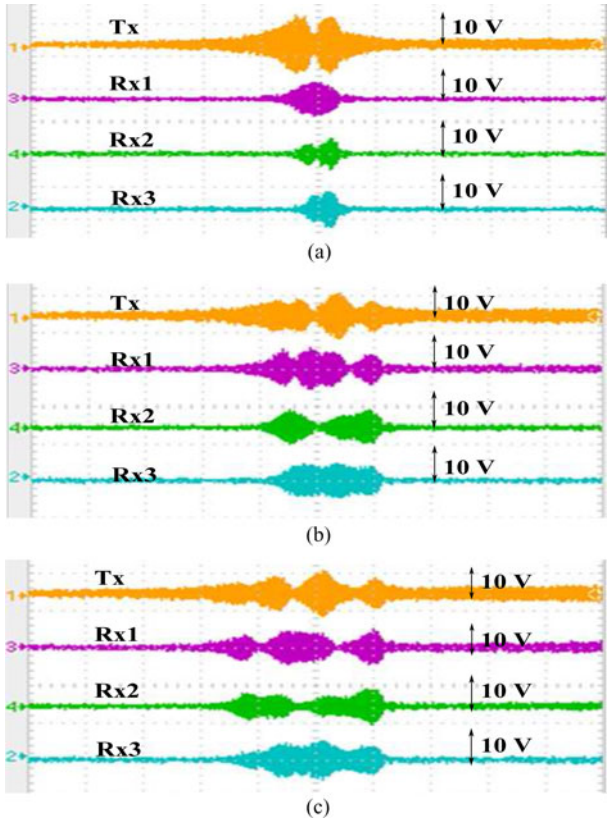

Fig. 11. Envelopes of signal in four-coil system. (a) refers to $k_{T1} = 0.0356,\ k_{T2} = 0.0019,\ k_{12} = 0.0021$ and $k_{23} = 0.0185$. (b) refers to $k_{T1} = k_{23}$ and $k_{T2} = k_{13}$. (c) refers to $k_{T1} = 0.144,\ k_{12} = 0.29,$ and $k_{23} = 0.54$.

we adopt a different view by utilzing the split frequencies as value added features. We assume that split frequency modes can be used to enhance system performance by deploying multiple splitting modes at different receivers. A receiver is tuned to the splitting frequency by using bandpass filters centred at each splitting frequency. The received power is proportional to the sum of the power at each splitting frequency. This method takes advantage of the frequency diversity and provides the received power as the following expression:

$$P_i = \sum_{1}^{N} P_N = \sum_{1}^{N} |I_i|_N^2 R_i \tag{14}$$

where N is the number of the splitting modes and I_i is the current of each resonator in (5). Equation (14) demonstrates the general case for calculating the received power at each type of mode. The power gain improvement of the received power

TABLE IV
RECEIVER POWER AND EFFICIENCY AT MODES 2 AND 3

Rx	Mode	Case	P_{ω_o} (dB)	P_{ω_2} (dB)	P_{ω_3} (dB)	P_i (dB)	Gain (%)
1	2	1	−20.1 (−20.8)	−9.05 (−9.03)	−9.04 (−9.03)	−6 (−6)	28.9 (29)
2	3	1	−6.17 (−6.17)	−12.16 (−12)	−12.1 (−12)	−4.39 (−4.4)	71.1 (71)
1	2	2	−26.7 (−26.7)	−9.03 (−9.05)	−9.03 (−9.05)	−6.02 (−6)	23 (23)
2	3	2	−6.06 (−6.05)	−12 (−12)	−12 (−12)	−4.3 (−4.3)	70.85 (71)

Cases 1 and 2 are with $k_{T1} = k_{12} = 0.2$ and $k_{T1} = k_{12} = 0.4$, respectively.
() denotes for analysing in LTspice.

between the splitting modes and the resonant frequency is calculated as Gain $= \frac{P_i}{P_{\omega_o}}$. Exact results of the receiver power at splitting frequency, resonant frequency, and power comparison are simulated using MATLAB and analyzed with ac analysis in LTspice.

Mode $N = 3$ (the case 1 in the SI2O System of Section III): Applying (14), the total powers at the receivers 1 and 2 are derived as follows:

$$\begin{aligned} P_1 &= (|I_1|^2_{\omega_2} + |I_1|^2_{\omega_3})R_i \\ P_2 &= (|I_2|^2_{\omega_1} + |I_2|^2_{\omega_2} + |I_2|^2_{\omega_3})R_i. \end{aligned} \tag{15}$$

It is noticed that the receivers 1 and 2 in (9) have two modes (ω_2, ω_3) and three modes $(\omega_1, \omega_2, \omega_3)$ of splitting frequency, respectively. However, these splitting frequencies are determined by the setting of the coupling coefficients. Therefore, using (9) and (15), the power of receivers 1 and 2 is computed with different values of the coupling coefficients as shown in Table IV.

It can be seen that both computation in MATLAB and LTspice show a similar result. There are two modes at receiver 1 and three modes at receiver 3, in which powers are obtained at P_{ω_2} and P_{ω_3} (two modes), and P_{ω_o}, P_{ω_2}, and P_{ω_3} (three modes). At $k = 0.2$, power gain at the two mode (−6 dB) and three mode (−4.39 dB) systems is improved by 28.9% and 71.1%, respectively, over the receiver power at the original resonant frequency (−20.1 and −6.17 dB). At $k = 0.4$, power efficiency increases by 23% in two modes $(\frac{-6\text{ dB}}{-26.7\text{ dB}})$ and 71% in three modes $(\frac{-4.3\text{ dB}}{-6\text{ dB}})$. It is also observed that received power P_{ω_o} at the original resonant frequency and given coupling in the three mode system is higher than in the two mode system.

Mode $N = 4$ (The Case 2 in the SI3O System of Section III): The method to calculate the received power is similar to that of mode $N = 3$, the total received powers at the receivers 1, 2, and 3 are obtained as follows:

$$\begin{aligned} P_1 &= (|I_1|^2_{\omega_1} + |I_1|^2_{\omega_2} + |I_1|^2_{\omega_3} + |I_1|^2_{\omega_4})R_i \\ P_2 &= (|I_2|^2_{\omega_1} + |I_2|^2_{\omega_2} + |I_2|^2_{\omega_3} + |I_2|^2_{\omega_4})R_i \\ P_3 &= (|I_3|^2_{\omega_1} + |I_3|^2_{\omega_2} + |I_3|^2_{\omega_3} + |I_3|^2_{\omega_4})R_i. \end{aligned} \tag{16}$$

In this case, we can see that the three receivers have the same splitting mode of 4, which are presented in (13). Using (13) and (16), the results of the received power at two coupling cases are shown in Table V. Again, similar results are gained

TABLE V
RECEIVER POWER AND EFFICIENCY AT MODE 4

Rx	Case	P_{ω_o} (dB)	P_{ω_1} (dB)	P_{ω_2} (dB)	P_{ω_3} (dB)	P_{ω_4} (dB)	P_i (dB)	Gain (%)
1	1	−15 (−15)	−13 (−13)	−12 (−12)	−12 (−12)	−13 (−13)	−6.4 (−6.4)	43 (43)
2	1	−30 (−30)	−13 (−13)	−13 (−13)	−13 (−13)	−13 (−13)	−7 (−7)	23 (23)
3	1	−16 (−16)	−17 (−17)	−9 (−9)	−9 (−9)	−17 (−17)	−5.3 (−5.3)	33 (33)
1	2	−20 (−20)	−13 (−13)	−13 (−13)	−13 (−13)	−13 (−13)	−7 (−7)	35 (35)
2	2	−42 (−42)	−13 (−13)	−13 (−13)	−13 (−13)	−13 (−13)	−7 (−7)	17 (17)
3	2	−21 (−21)	−17 (−17)	−9 (−9)	−9 (−9)	−17 (−17)	−5.3 (−5.3)	25 (25)

Case 1 and case 2 are with $k_{T1} = k_{12} = k_{23} = 0.2$ and $k_{T1} = k_{12} = k_{23} = 0.4$, respectively.
() denotes for analysing in LTspice.

in MATLAB and LTspice. At a given coupling case, the total power at four-splitting mode is compared with the power at the resonant frequency. It is shown that in case 1, power gain is increased to 43% $(\frac{-6.4\text{ dB}}{-15\text{ dB}})$, 23% $(\frac{-7\text{ dB}}{-30\text{ dB}})$, and 33% $(\frac{-5.3\text{ dB}}{-16\text{ dB}})$ in receivers 1, 2, and 3, respectively.

We have demonstrated the received power of the two- and three-splitting mode in three-coil model and four-splitting in four-coil model. This can be concluded that under a particular coupling condition, several splitting modes can be produced to enable the improvement of the power transfer capacity. This method can be applied to a number of receiver coils in wireless-powered capsule in medical implant device. For example, in implant, we can layout antenna coils along capsule in a manner that the system can create multiple modes when the transmitter transfers energy from outside. The use of splitting mode from the array of antenna coil along the capsule could help to enhance the received power. Furthermore, the cooperative location between the receivers can create 2-D or 3-D antenna configuration. The splitting frequencies can be calculated from any position of receivers. Therefore, it may have a free location of receiver side compared to a single antenna. The advantage of the multiple splitting mode and 3-D configuration is the ability to power multiple receivers at the same time. Note that the design of the peak power detector at receivers is not within the scope of this paper. Further investigation on a new form of the antenna configuration adapted from the multiple splitting modes and optimal control of the peak power will be our future research.

VII. CONCLUSION

We have demonstrated the one, two, three, and four modes of the splitting frequency in this paper. The theoretical and experimental results validate the splitting frequencies in different situations. The splitting frequency phenomenon is affected by the mutual coupling behavior between the resonators and can be obtained from the eigenvalues of the matrix equation. In addition, the spectral response and voltage excitation experimentally verify the splitting mode in each receiver, which uses frequency diversity transmissions of the receivers. Furthermore, multiple frequencies can be achieved from the splitting system. The more the number of coils at critical couplings, the more is the number

of splitting frequencies. Consequently, the multiple modes of splitting frequency could be used to enhance the received power by aggregating the power at different frequencies.

REFERENCES

[1] A. Kurs, A. Karalis, R. Moffatt, J. D. Joannopoulos, P. Fisher, and M. Soljacić, "Wireless power transfer via strongly coupled magnetic resonances," *Science*, vol. 317, no. 5834, pp. 83–86, 2007.

[2] A. Sample, B. Waters, S. Wisdom, and J. Smith, "Enabling seamless wireless power delivery in dynamic environments," *Proc. IEEE*, vol. 101, no. 6, pp. 1343–1358, Jun. 2013.

[3] Y.-H. Kim, S.-Y. Kang, S. Cheon, M.-L. Lee, and T. Zyung, "Wireless charging technology using magnetically coupled resonators," in *Proc. IEEE 33rd Int. Telecommun. Energy Conf.*, Oct. 2011, pp. 1–3.

[4] M. Kato, T. Imura, and Y. Hori, "New characteristics analysis considering transmission distance and load variation in wireless power transfer via magnetic resonant coupling," in *Proc. IEEE 34th Int. Telecommun. Energy Conf.*, Sep. 2012, pp. 1–5.

[5] N. Shinohara, "Wireless power transmission progress for electric vehicle in japan," in *Proc. IEEE Radio Wireless Symp.*, Jan. 2013, pp. 109–111.

[6] N. Liu and T. Habetler, "Design of a universal inductive charger for multiple electric vehicle models," *IEEE Trans. Power Electron.*, to be published.

[7] X. Liu, F. Zhang, S. Hackworth, R. Sclabassi, and M. Sun, "Wireless power transfer system design for implanted and worn devices," in *Proc. IEEE 35th Annu. Northeast Bioeng. Conf.*, Apr. 2009, pp. 1–2.

[8] K. Lee and D.-H. Cho, "Maximizing the capacity of magnetic induction communication for embedded sensor networks in strongly and loosely coupled regions," *IEEE Trans. Magn.*, vol. 49, no. 9, pp. 5055–5062, Sep. 2013.

[9] Z. Sun and I. Akyildiz, "Magnetic induction communications for wireless underground sensor networks," *IEEE Trans. Antennas Propag.*, vol. 58, no. 7, pp. 2426–2435, Jul. 2010.

[10] J. Agbinya and S. Lal, "A high capacity near-field inductive coupled miso communication system for internet of things," in *Proc. 6th Int. Conf. Broadband Biomed. Commun*, Nov. 2011, pp. 112–117.

[11] F. Zhang, S. Hackworth, W. Fu, C. Li, Z. Mao, and M. Sun, "Relay effect of wireless power transfer using strongly coupled magnetic resonances," *IEEE Trans. Magn.*, vol. 47, no. 5, pp. 1478–1481, May 2011.

[12] J. Kim, H.-C. Son, K.-H. Kim, and Y.-J. Park, "Efficiency analysis of magnetic resonance wireless power transfer with intermediate resonant coil," *IEEE Antennas Wireless Propag. Lett.*, vol. 10, pp. 389–392, May 2011.

[13] C. K. Lee, W. Zhong, and S. Y. R. Hui, "Effects of magnetic coupling of nonadjacent resonators on wireless power domino-resonator systems," *IEEE Trans. Power Electron.*, vol. 27, no. 4, pp. 1905–1916, Apr. 2012.

[14] J. I. Agbinya and N. F. A. Mohamed, "Design and study of multi-dimensional wireless power transfer transmission systems and architectures," *Int. J. Electr. Power Energy Syst.*, vol. 63, pp. 1047–1056, 2014.

[15] H. Nguyen, J. I. Agbinya, and J. Devlin, "Channel characterisation and link budget of MIMO configuration in near field magnetic communication," *Int. J. Electron. Telecommun.*, vol. 59, pp. 255–262, 2013.

[16] Y. Zhang, T. Lu, Z. Zhao, F. He, K. Chen, and L. Yuan, "Employing load coils for multiple loads of resonant wireless power transfer," *IEEE Trans. Power Electron.*, to be published.

[17] D. Ahn and S. Hong, "Effect of coupling between multiple transmitters or multiple receivers on wireless power transfer," *IEEE Trans. Ind. Electron.*, vol. 60, no. 7, pp. 2602–2613, Jul. 2013.

[18] B. Cannon, J. Hoburg, D. Stancil, and S. Goldstein, "Magnetic resonant coupling as a potential means for wireless power transfer to multiple small receivers," *IEEE Trans. Power Electron.*, vol. 24, no. 7, pp. 1819–1825, Jul. 2009.

[19] A. Kurs, R. Moffatt, and M. Soljacć, "Simultaneous mid-range power transfer to multiple devices," *Appl. Phys. Lett.*, vol. 96, no. 4, p. 044102, Jan. 2010.

[20] U. Azad, H. Jing, and Y. Wang, "Link budget and capacity performance of inductively coupled resonant loops," *IEEE Trans. Antennas Propag.*, vol. 60, no. 5, pp. 2453–2461, May 2012.

[21] W.-Q. Niu, J.-X. Chu, W. Gu, and A.-D. Shen, "Exact analysis of frequency splitting phenomena of contactless power transfer systems," *IEEE Trans. Circuits Syst. I, Reg. Papers*, vol. 60, no. 6, pp. 1670–1677, Jun. 2013.

[22] W. Niu, W. Gu, J. Chu, and A. Shen, "Coupled-mode analysis of frequency splitting phenomena in cpt systems," *Electron. Lett.*, vol. 48, no. 12, pp. 723–724, Jun. 2012.

[23] Y. Zhang and Z. Zhao, "Frequency splitting analysis of two-coil resonant wireless power transfer," *IEEE Antennas Wireless Propag. Lett.*, vol. 13, pp. 400–402, Feb. 2014.

[24] Y. Zhang, Z. Zhao, and K. Chen, "Frequency-splitting analysis of four-coil resonant wireless power transfer," *IEEE Trans. Ind. Appl.*, vol. 50, no. 4, pp. 2436–2445, Jul./Aug. 2014.

[25] A. Trigui, S. Hached, F. Mounaim, A. Ammari, and M. Sawan, "Inductive power transfer system with self-calibrated primary resonant frequency," *IEEE Trans. Power Electron.*, to be published.

[26] D. Ahn and S. Hong, "A study on magnetic field repeater in wireless power transfer," *IEEE Trans. Ind. Electron.*, vol. 60, no. 1, pp. 360–371, Jan. 2013.

[27] O. Karaca, F. Kappeler, D. Waldau, R. Kennel, and J. Rackles, "Eigenmode analysis of a multiresonant wireless energy transfer system," *IEEE Trans. Ind. Electron.*, vol. 61, no. 8, pp. 4134–4141, Aug. 2014.

[28] H. Nguyen, J. Agbinya, and J. Devlin, "FPGA-Based implementation of multiple modes in near field inductive communication using frequency splitting and MIMO configuration," *IEEE Trans. Circuits Syst. I, Reg. Papers*, vol. 62, no. 1, pp. 302–310, Jan. 2015.

[29] H. Wheeler, "Simple inductance formulas for radio coils," *Proc. Inst. Radio Eng.*, vol. 16, no. 10, pp. 1398–1400, Oct. 1928.

Hoang Nguyen (S'11) received the M.E. degree in communication from La Trobe University, Melbourne, Australia, in 2003, where he is currently working toward the Ph.D. degree in electronics and communication engineering.

From 2003 to 2011, he was with Vietnam Telecom International, where he was a Telecom Network Specialist participating in design, development, and implementation of VoIP network, VSAT network, contact centre, voice, Internet, VPN, Lease line, video conferencing, mobile trunking over VSAT Network, signaling transfer protocol, and next generation network. His current research interests include wireless power transfer, near-field communication, body area network, and internet of things.

Johnson I. Agbinya received the B.Sc. degree in electronic/electrical engineering from Obafemi Awolowo University (OAU), Ife Nigeria, M.Sc. (Research) degree in electronic control from the University of Strathclyde Glasgow Scotland, and Ph.D. degree in microwave radar systems from La Trobe University, Melbourne Australia.

He is currently the Head with the School of Information Technology and Engineering, Melbourne Institute of Technology, Melbourne, VIC, Australia. Prior to that, he was an Associate Professor with the Department of Electronic engineering, La Trobe University, Melbourne. He is also an Honorary Professor at the University of Witwatersrand, Johannesburg, South Africa, Extraordinary Professor at the University of the Western Cape, Cape Town, South Africa, and the Tshwane University of Technology, Pretoria, South Africa. Prior to joining La Trobe University in November 2011, he was Senior Research Scientist with CSIRO Telecommunications and Industrial Physics (now CSIROICT) from 1993 to 2000, Principal Research Engineering with Vodafone Australia from 2000 to 2003, and Senior Lecturer with UTS Australia from 2003 to 2011. His research interests include remote sensing, internet of things (machine to machine communications), biomonitoring systems, wireless power transfer, mobile communications, and biometrics systems. He has authored/coauthored nine books in telecommunications, some of which are used as textbooks. He is the Founder of the International Conference on Broadband Communications and Biomedical Applications, Pan African Conference on Science, Computing and Telecommunications, and the *African Journal of Information and Communication Technology*.